RSC Advances

PAPER

View Article Online
View Journal | View Issue

Cite this: *RSC Adv.*, 2025, **15**, 7191

Enhancing diabetes therapy with pH-sensitive co-delivery of metformin hydrochloride and glipizide using MCM-48-based dual drug delivery system

Debatrayee Dasgupta and Anjali Patel *

Received 8th January 2025
Accepted 21st February 2025

DOI: 10.1039/d5ra00204d

rsc.li/rsc-advances

Monotherapy in diabetes management is losing interest due to its ineffectiveness in achieving optimal glycaemic control in a significant proportion of diabetic patients. Therefore, combined therapy is increasingly preferred by clinicians, which offers enhanced effectiveness and a better safety profile for managing the condition. The present work deals with the designing of a dual drug nanocarrier based on MCM-48 and 12-tungtophosphoric acid (TPA) for the co-delivery of Glipizide (GLP) and Metformin Hydrochloride (MTF) as well as its characterization using various techniques. An *in vitro* release study was carried out at two different pHs (pH 1.2 and pH 7.4) at 37 °C under stirring conditions which was further supported by an *in vitro* dissolution study carried out using a USP Type II dissolution apparatus. The obtained results were compared with that of the marketed available formulation, Glirum-MF, and the designed nanocarrier showed a better controlled release of both the drugs in comparison with the conventional drug. Additionally, considering the anticancer properties of both the drugs, MTT assay indicated that the carrier is non-toxic while the drug loaded nanocarrier shows apoptosis against HepG2 cells.

Introduction

Type 2 diabetes mellitus (T2DM) represents a significant global public health challenge, with an alarming rise in incidence, particularly in developing nations. This condition is among the most formidable health issues of the 21st century.[1] The primary pathophysiology of T2DM involves insulin resistance combined with inadequate insulin release from β-cell, leading to elevated blood glucose levels known as hyperglycaemia. Prolonged hyperglycaemia can result in the glycation of proteins, which subsequently contributes to a variety of secondary complications, including retinopathy, cardiovascular disease, diabetic foot, neuropathy, and nephropathy. As a result, individuals may experience a decline in quality of life, along with an increased risk of disability and mortality.[2,3]

Anti-diabetic drugs are designed to maintain normal blood glucose levels by reducing plasma glucose concentrations. In comparison to injectable insulin formulations, oral anti-diabetic drugs are increasingly preferred by healthcare professionals due to their ease of administration and enhanced control over blood glucose levels.[4] However, clinical studies indicate that administering a single dose to diabetic patients may not be optimal, rather, employing double or multiple combination dosing has demonstrated greater efficacy. An effective treatment strategy for T2DM includes the utilization of an insulin sensitizer alongside an insulin secretagogue, while considering the underlying pathophysiology of the disease. In this direction, the combination of Metformin Hydrochloride (MTF) and Glipizide (GLP) neither increases fasting insulin levels or body weight, nor does it have a substantial impact on lipid profiles. Therefore, this combination represents a safe, effective, and cost-efficient therapeutic option for T2DM patients responding adequately to monotherapy.[5,6]

MTF and GLP are oral hypoglycaemic agents belonging to the biguanide and sulfonylurea class respectively, primarily employed in the management of T2DM. MTF operates by decreasing hepatic glucose production and enhancing insulin sensitivity through increased peripheral glucose uptake. Due to its relatively short and variable biological half-life of 1.5–4.5 h, MTF is typically administered 2–3 times with a common regimen of 250 mg per day to maintain effective plasma concentrations. GLP, on the other hand, reduces glucose levels by stimulating insulin secretion from pancreatic β-cells. With a similar biological half-life of 2–4 h, the recommended dosage is 2.5 mg with 2–3 times of administration daily depending on the patient. The combination of MTF and GLP has been shown to be more effective than monotherapy, owing to the synergistic effects of the two agents.[7,8]

The complementary effect associated with the combination of MTF and GLP highlights significant advantages. In this direction, a literature survey shows that different type of controlled nanocarriers including osmotic pumps, niosomes, liposomes, polymers[4,9–14] have been used for the co-delivery of

Department of Chemistry, Faculty of Science, The Maharaja Sayajirao University of Baroda, Vadodara, 390002, India. E-mail: anjali.patel-chem@msubaroda.ac.in

MTF and GLP. Although these materials can deliver drugs in a sustained manner, but the major concern is the structural degradation of such carriers under various physiological conditions which leads to premature release of the drug.[15,16] Thus, the increasing demand for structurally stable carriers has driven research into inorganic nanoparticle platforms, particularly the Mesoporous Silica Nanoparticles (MSNs).

MSNs have emerged as a prominent nanocarrier due to their unique properties which include the ability to tune particle size and morphology, achieve uniform and adjustable pore sizes, and provide high surface area as well as pore volume.[17] Additionally, MSNs allow facile surface functionalization and exhibit stable physicochemical characteristics. The M41-S family consists of the one-dimensional hexagonal MCM-41, the three-dimensional cubic MCM-48, and the less stable lamellar MCM-50. Among these, the hexagonal MCM-41 has garnered the most attention in drug delivery due to its availability and reproducibility. In contrast, the cubic MCM-48 nanoparticles (nMCM-48), which features three-dimensional channels, has received comparatively less focus, with no existing reports regarding its potential as a carrier for the co-delivery of MTF and GLP.[18–21]

Thus, in quest of an efficient nanocarrier for co-delivery of two antidiabetic agents, a nanocarrier was designed using nMCM-48 along with 12-tungstophosphoric acid (TPA) as a capping agent (Scheme 1). TPA, recognized as a Keggin type of polyoxometalate (POM), is known for its medical applications.[22] Notably, it is reported that tungstate can enhance pancreatic β-cell function and promote insulin secretion in small animal models.[23–25] The synthesized dual nanocarrier was thoroughly characterized using various physicochemical techniques. An *in vitro* release study was performed in both Simulated Body Fluid (SBF) and Simulated Gastric Fluid (SGF), with the resultant release profile being compared to that of the commercially available formulation, Glirum-MF. This analysis was further substantiated by an *in vitro* dissolution study utilizing a USP type II dissolution apparatus. Additionally, in light of the anticancer potential of both drugs and the elevated risk of cancer in patients with T2DM, the anticancer efficacy of MTF and GLP against HepG2 cell line was assessed through an MTT assay.

The present work involves the following several noteworthy elements, including:

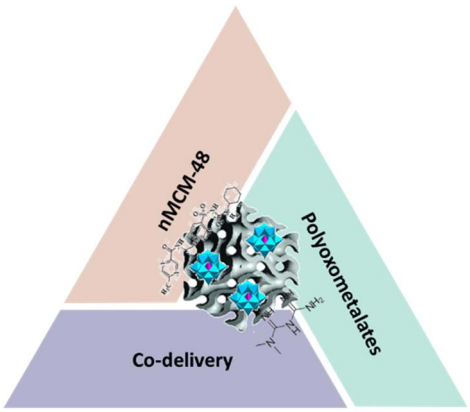

Scheme 1 Schematic representation of the work carried out.

(i) The first novel nanocarrier based on MCM-48 for the co-delivery of MTF and GLP.

(ii) This study marks the first application of the inorganic moiety TPA as a capping agent.

(iii) Furthermore, both drugs not only exhibit promising antidiabetic therapeutic effects but also possess the potential to address cancer, which is particularly beneficial for patients with T2DM given their increased risk of cancer and cancer-related mortality.

Experimental

Materials

All chemicals were of A.R. grade and used without further purification. Cetyltriethylammoniumbromide (CTAB) was received from Lobachemie, Mumbai. 12-Tungstophosphoric acid (TPA), tetraethylorthosilicate (TEOS), ethanol and liquor ammonia (25%) were procured from Merck. Glipizide (GLP) and Metformin Hydrochloride (MTF) were obtained from Sigma Aldrich. Glirum-MF, a commercially available formulation consisting of GLP (5 mg active amount) and MTF (500 mg active amount) was purchased from medical store. Human hepatocellular liver carcinoma (HepG2) cell line was procured from National Centre for Cell Science, Pune, India.

Preparation of the release medium

Two different release media were prepared, *viz.*, Simulated Body Fluid (SBF, pH 7.4) and Simulated Gastric Fluid (SGF, pH 1.2), representing the human physiological pH and acidic environment. SGF was prepared by dissolving 6.2 g of concentrated HCL in 1000 mL distilled water while SBF was prepared by dissolving 72.5 mg of Na_2HPO_4, 12.5 mg of KH_2PO_4, 10.7 mg of KCl, and 400 mg of NaCl in 250 mL of distilled water.

Designing of dual drug nanocarrier

The synthesis was carried out in two steps as shown in Scheme 2:

Step 1: synthesis of nMCM-48 and encapsulation of GLP (GLP/nMCM-48). The nMCM-48 was synthesized by a base-catalyzed sol–gel process as reported previously by our group.[26] In a nutshell, 2.4 g of CTAB surfactant was added to 50 mL of distilled water and allowed to dissolve completely at 35 °C. Then, 50 mL of ethanol and 15.4 mL of 25% wt liquor ammonia were added to this solution and stirred for 15–20 min followed by the dropwise addition of 3.4 g TEOS. The resulting white suspension was stirred for 2 h, filtered, and washed. The obtained material was dried at room temperature and calcined at 550 °C for 6 h.

GLP encapsulation was carried out using previously reported method.[27] A 1.0 mg mL^{-1} solution was made by dissolving

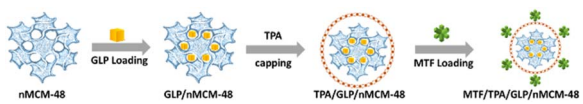

Scheme 2 Schematic illustration of the synthesis process.

20 mg of GLP in 20 mL of a 70 : 30 water–methanol mixture. In this solution, 20 mg of nMCM-48 was suspended and sonicated for 10 min for uniform dispersion, then stirred for 24 h at 37 °C for effective drug loading. After completion of 24 h, the particles were isolated *via* ultracentrifugation, washed twice with acetone to remove excess drug, air-dried, and stored. The obtained material was designated as GLP/nMCM-48.

Step 2: capping of GLP/nMCM-48 with 12-tungstophosphoric acid (TPA) and loading of MTF. By using the previously reported procedure,[27] GLP/nMCM-48 was capped with TPA using the incipient wet impregnation method. 1 g of GLP/nMCM-48 was impregnated using 30% aqueous solution of TPA (0.3 g in 30 mL of distilled water). The resulting material was designated as TPA/GLP/nMCM-48. Further, the loading of MTF was performed using the soaking method. First, 20 mg of TPA/GLP/nMCM-48 was ultrasonically dispersed in 20 mL of a MTF solution (0.1 mg mL^{-1} in distilled water) for 10 min to ensure uniform mixing. The resulting suspension was then stirred at room temperature for 24 h and after completion, the nanoparticles were isolated by ultracentrifugation, and the supernatant was separated. The drug-loaded nanoparticles were washed twice with acetone to remove any unbound drug and air-dried. The obtained material was designated as MTF/TPA/GLP/nMCM-48.

Characterization

The FT-IR spectra were recorded on a PerkinElmer instrument using KBr in the wavelength range of 400–4000 cm^{-1}. A JSM 5610 LV EDS-SEM analyser was used for the SEM analysis having an accelerating voltage of 15 kV, a working distance of 1 mm, and backscattered electron detectors along with an EDS system. A gold coating was used to enhance the imaging quality. A JEOL TEM instrument (model-JEM 2100) with a 200 kV acceleration voltage and a carbon-coated 200 mesh Cu grid was used for transmission electron microscopy (TEM). TGA were performed using a TG–DTA 6300 INCARP EXSTAR 6000 in the temperature range of 30–500 °C with a heating rate of 10 °C min^{-1} and throughout the measurement a nitrogen atmosphere was maintained. The detailed characterizations related to nMCM-48, GLP/nMCM-48 and TPA/GLP/nMCM-48 are already published by our group;[26–28] however, for comparison and the reader's convenience some of the characterizations are included here as well.

In vitro drug release study

The release behaviour of GLP and MTF was evaluated in pH 7.4 and pH 1.2. 5 mg of MTF/TPA/GLP/nMCM-48 was suspended in 10 mL solution of the release media and stirred continuously at a temperature of 37 °C. At fixed time intervals, aliquots were obtained and were replenished using equal volume of fresh release media. Using a PerkinElmer Lambda 35 UV-visible spectrophotometer, the absorbance was recorded at 274 nm (GLP) and 234 nm (MTF). The concentrations of GLP as well as MTF in the release media were determined according to the standard curves of each drug at corresponding pH and the cumulative drug release percentages were plotted against time.

The % entrapment efficiency and % loading capacity was calculated for both the drugs using the following equation:

$$\%\ \text{Entrapment efficiency} = \frac{I_c - I_s}{I_c} \times 100$$

where, I_c indicates the initial concentration of the drug taken, while I_s indicates the concentration of drug in supernatant.

While the % loading capacity for both the drugs was calculated using the following equation:

$$\%\ \text{Loading capacity} = \frac{\text{Weight of drug loaded}}{\text{Total weight of nanocarrier}} \times 100$$

In vitro dissolution study

The *in vitro* dissolution studies were carried out using a USP type II apparatus (paddle). The dissolution medium (SBF or SGF) was transferred into the dissolution jar and the assembly was maintained at 37 ± 0.5 °C. After attaining the set temperature, 5 mg of the sample was introduced and the medium was stirred at 150 rpm. 3 mL of the sample was withdrawn at fixed time interval and was refilled with the same volume of fresh media. The drug release at different time intervals was measured using an UV-visible spectrophotometer as mentioned above.

In vitro cytotoxicity-MTT assay

The MTT assay is a widely used colorimetric method for assessing cell viability and cytotoxicity, particularly in the context of evaluating the efficacy of nanocarriers. The cells viability was accessed *via* MTT assay against the human hepatocellular carcinoma (HepG2) cell lines which were maintained in a CO_2 incubator with 5% CO_2 and 95% humidity atmosphere. The cells (10^5) were then developed in a T25 flask, cultured in DMEM with 10% FBS and 1% antibiotic–antimycotic solution, trypsinised every 72 h, and subcultured with a TPVG solution. A 96 well-culture plates were seeded with 7×10^3 cells per well was made to proliferate overnight and then subsequently treated with compounds under investigation at doses ranging from 25 to 500 μg mL^{-1}. Following that, 100 mL of MTT was added to each well, and the wells were incubated for 4 h at 37 °C. Post treatment, the formazan was dissolved in 150 mL of DMSO and the absorbance was measured at 540 nm through multiwall micro-plate reader (Synergy HTX Bio Tek Instruments, Inc., Winooski, VT). The untreated or control cells were also employed as reference and to run with the same conditions. The value of maximum absorbance depends upon the employed solvent in sample solution and the percentage (%) viability of cells was calculated as per the mentioned below equation:

$$\%\ \text{Viability} = \frac{\text{Total cells} - \text{viable cells}}{\text{Total cells}} \times 100$$

Results and discussion

Characterization

The FT-IR spectrum of nMCM-48 (Fig. 1) exhibits a broad band in the range of 1100–1250 cm^{-1}, attributed to the asymmetric stretching of Si–O–Si bonds. Additional bands are observed at

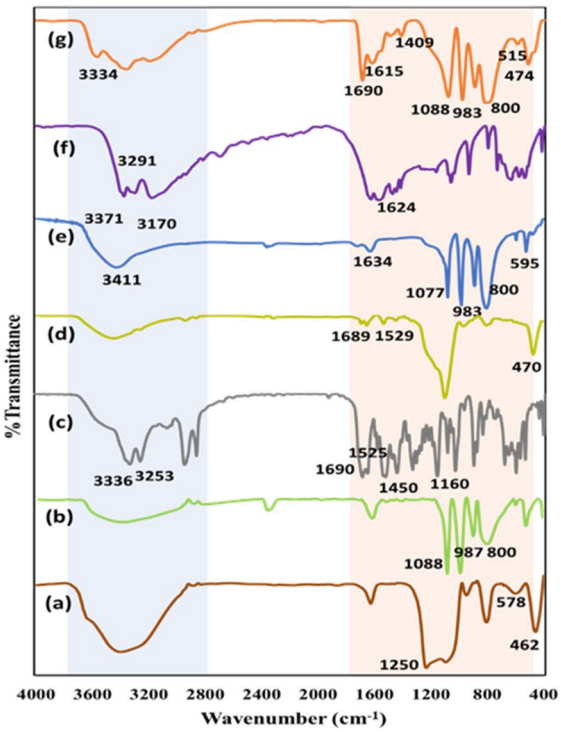

Fig. 1 FT-IR spectra of (a) nMCM-48, (b) TPA, (c) GLP, (d) GLP/nMCM-48, (e) TPA/GLP/nMCM-48 (f) MTF and (g) MTF/TPA/GLP/nMCM-48.

578 cm^{-1} and 462 cm^{-1}, corresponding to the symmetric stretching of Si–O–Si and the bending vibration of Si–O, respectively.[28] In the case of GLP/nMCM-48, the spectrum display bands at 470 cm^{-1}, 1529 cm^{-1}, and 1689 cm^{-1}, which correspond to the Si–O bending vibration of nMCM-48, C=O stretching, and aromatic vibrations of GLP.[27] The slight shifts in these bands confirm the successful incorporation of GLP into the nMCM-48 structure. The spectra of TPA/GLP/nMCM-48, characteristic peaks of nMCM-48 are noted at 579 cm^{-1} and 476 cm^{-1}, corresponding to the symmetric stretching of Si–O–Si and Si–O bending vibrations, both exhibiting minor shifts. Characteristic peaks are observed at 545, 1077 and 1634 corresponding to the symmetric stretching of Si–O–Si and P–O as well as C=O present in nMCM-48, TPA and GLP respectively. Additionally, a slight shift in these characteristic peaks indicates the effective bonding between TPA and GLP. In the spectrum of MTF/TPA/GLP/nMCM-48, a band appears around 1615 cm^{-1} with reduced intensity and a slight shift compared to the 1624 cm^{-1} band of MTF[29] which suggests the successful loading of MTF and its interaction with TPA.

According to the SEM micrographs as shown in Fig. 2, all the synthesized materials have uniform particle size distribution. The nanocarriers measured between 270 and 370 nm in size. The average particle size of nMCM-48, GLP/nMCM-48, TPA/GLP/MCM-48 and MTF/TPA/GLP/nMCM-48 was found to be 272.9 ± 6.2 nm, 290.9 ± 6.8 nm, 309.3 ± 9.8 nm and 366.7 ± 26.2 nm respectively. The corresponding particle size histograms are shown in Fig. 3.

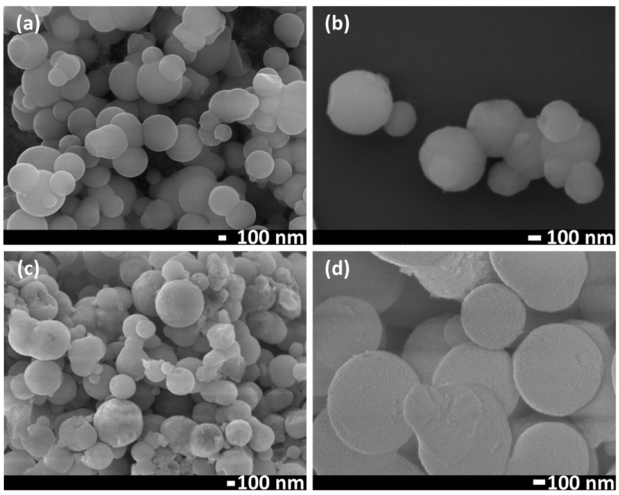

Fig. 2 SEM images of (a) nMCM-48, (b) GLP/nMCM-48, (c) TPA/GLP/MCM-48 and (d) MTF/TPA/GLP/nMCM-48.

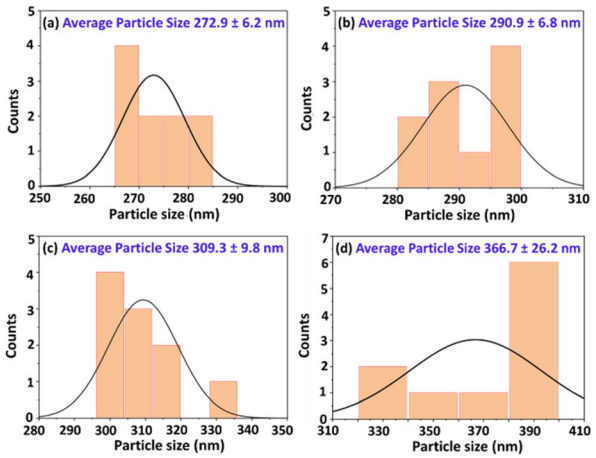

Fig. 3 Histograms showing the particle size distribution pattern for the corresponding SEM images of (a) nMCM-48, (b) GLP/nMCM-48, (c) TPA/GLP/MCM-48 and (d) MTF/TPA/GLP/nMCM-48.

The gradual increase in the average particle size shows the successful loading of both the drugs as well as capping with TPA. The spherical morphology of nMCM-48 is retained even after drug loading and capping, showing the uniform dispersion of both MTF, GLP as well as TPA. This is further supported by the TEM images.

The TEM images (Fig. 4) of nMCM-48, GLP/nMCM-48 and MTF/TPA/GLP/nMCM-48 were recorded at various magnifications. In case of nMCM-48, the images show well-ordered pore networks with uniform particle diameter. More opaque pores were observed in case of GLP/nMCM-48 and MTF/TPA/GLP/nMCM-48 compared to nMCM-48 showing that the pores are uniformly filled with both the drugs and successfully capped with TPA without any agglomeration.

The TGA analysis of nMCM-48 (Fig. 5) indicates an initial weight loss of 8.9% up to 110 °C, which is attributed to the removal of physically adsorbed water molecules. A further

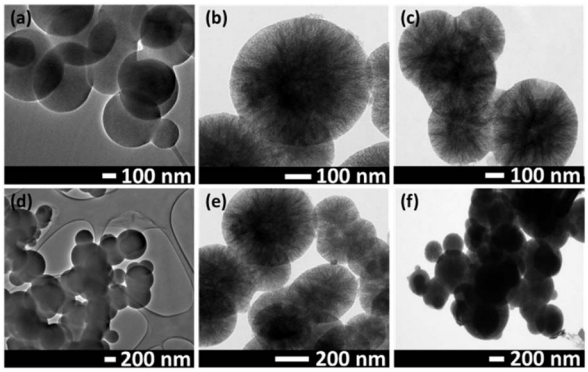

Fig. 4 TEM images of (a and d) nMCM-48, (b and e) GLP/nMCM-48, and (c and f) MTF/TPA/GLP/nMCM-48.

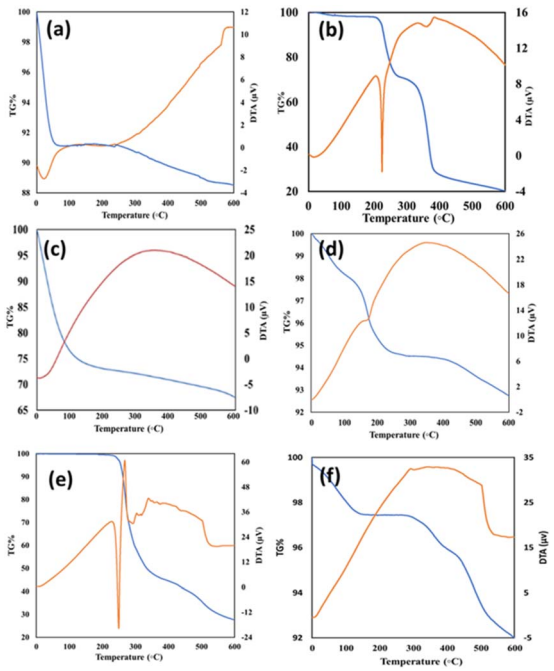

Fig. 5 TG–DTA curves of (a) nMCM-48, (b) GLP, (c) GLP/nMCM-48, (d) TPA/GLP/nMCM-48, (e) MTF and (f) MTF/TPA/GLP/nMCM-48.

minimal weight loss, less than 1%, occurs up to 400 °C, likely due to the condensation of silanol groups within the material. For the pure drug GLP, a distinct endothermic peak is observed at 207 °C,[27] corresponding to its melting point. In the case of GLP/nMCM-48, this endothermic peak is significantly diminished, suggesting strong interactions between the drug and the carrier, leading to a broader, less intense peak. The DTA profile for pure MTF initially shows a stable baseline, followed by a prominent endothermic peak at 230 °C, representing the volatilization of hydrogen chloride and the $C_4N_3H_7$ fragment. An exothermic peak at 255 °C (ref. 30) follows, corresponding to the decomposition and release of the H_4N_2 fragment. For MTF/TPA/GLP/nMCM-48, both the endothermic and exothermic peaks of MTF are noticeably reduced, indicating effective drug loading and interaction with the carrier material.

Table 1 % entrapment efficiency of MTF and GLP

Drugs	MTF	GLP
% entrapment efficiency	91.0	80.0
% loading capacity	45.5	40.0

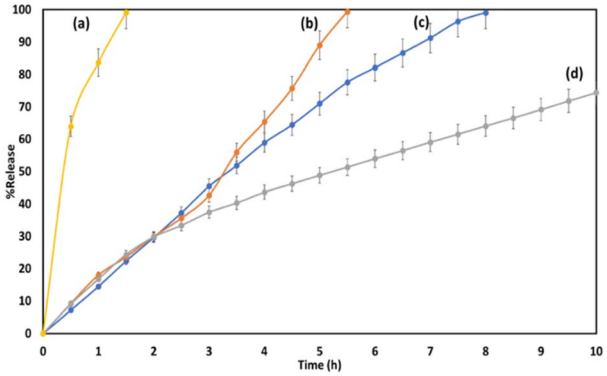

Fig. 6 *In vitro* release profile of GLP at (a) pH-7.4, (b) pH-1.2 and MTF at (c) pH-1.2 and (d) pH-7.4.

In vitro drug release study

The percentage of successfully entrapped as well as loaded GLP and MTF into the designed nanocarrier was determined using a UV-visible spectrophotometer as shown in Table 1. The entrapment efficiency of GLP is lower than MTF because of the terminal oxygen present in TPA which binds with larger amount MTF. On the contrary, in case of GLP since it is directly loaded into the pores of nMCM-48, such type of interactions is not possible.

Effect of pH on release study

The release studies were conducted in two different media: acidic (pH 1.2) and basic (pH 7.4) and the cumulative release of MTF and GLP was measured over a specified period as well as the results were quantitatively analysed as shown in Fig. 6.

The obtained result indicates that GLP (Table 2) exhibits a slower release profile in acidic conditions (pH 1.2). A burst release in the release profile of GLP is obtained in case of pH 7.4 with almost 99% of the drug being released at the end of 1.5 h. The reason behind this burst release could be due to polarization of the sulfonyl and carbonyl groups present in GLP (weak acid, pK_a value of 5.9)[31] which makes it less soluble in acidic medium resulting in an initial 36% and 99.3% of the drug release at the end of 2.5 h and 5.5 h respectively in pH 1.2.

Table 2 Effect of pH on the release of GLP and MTF

	% release		
Drug	pH 1.2	pH 7.4	Release rate
MTF	99.9 (8 h)	74.3 (10 h)	Slower release obtained in basic pH
GLP	99.3 (5 h)	99.9 (1.5 h)	Slower release obtained in acidic pH

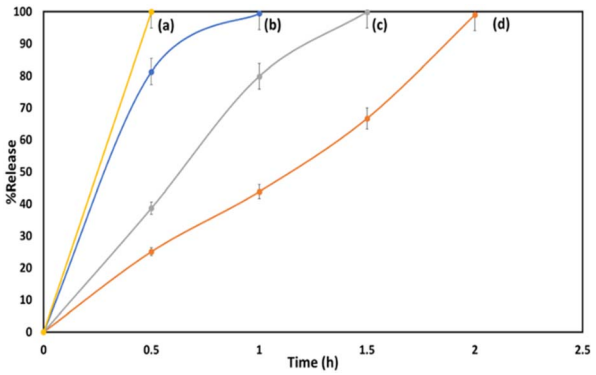

Fig. 7 *In vitro* release profile of GLP at (a) pH-7.4, (d) pH-1.2 and MTF at (b) pH-1.2, (c) pH-7.4 from the marketed drug.

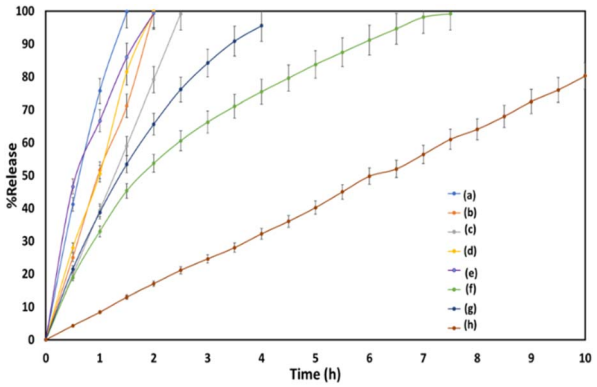

Fig. 8 *In vitro* dissolution profile of GLP at (a) pH-7.4, (b) pH-1.2 and MTF at (d) pH-1.2, (c) pH-7.4 from Glirum-MF as well as *in vitro* dissolution profile of GLP at (e) pH-7.4, (f) pH-1.2 and MTF at (g) pH-1.2, (h) pH-7.4 from MTF/TPA/GLP/nMCM-48.

On the contrary, the data also shows that the release of MTF is significantly slower in basic medium compared to the acidic with 99% of the drug being release at the end of 8 h at pH 1.2 while at pH 7.4, 74% of the drug is release at the end of 10 h. The slower release is primarily due to the stability of TPA in acidic pH, where the capping remains intact. In contrast, at basic pH, the capping becomes less effective at controlling the release, leading to a higher amount of drug release at pH 7.4.

Therefore, the overall release study suggests a pH-dependent release behaviour in case of both the hydrophobic (GLP) and the hydrophilic drug (MTF) that can be advantageous for therapeutic applications.

Comparison with marketed available drug, Glirum-MF

Fig. 7 shows the *in vitro* drug release profile obtained for MTF and GLP at pH 1.2 and pH 7.4 from the marketed drug, Glirum-MF. The obtained result shows that 99% of MTF was released within 1 h and 1.5 h at pH 1.2 and pH 7.4 respectively. At pH 1.2, 99% of GLP was released after 2 h while at pH 7.4, 99% was released within 0.5 h.

It can be observed from Fig. 6 and 7 that significantly slower and more effective release compared is obtained in case of MTF/TPA/GLP/nMCM-48. In contrast to the marketed drug, the designed nanocarrier not only improves bioavailability of both MTF and GLP but also minimizes the frequency of dosing, thereby enhancing patient compliance.

In vitro dissolution study

The *in vitro* release study described above was further supported by an *in vitro* dissolution study carried out using a USP type II dissolution apparatus for both MTF/TPA/GLP/nMCM-48 as well as the marketed drug at pH 1.2 and pH 7.4. The obtained results are shown in Fig. 8.

The results obtained from *in vitro* dissolution study also supports the fact that slower and better release of GLP and MTF are obtained in pH 1.2 and 7.4 respectively from MTF/TPA/GLP/nMCM-48 compared to Glirum-MF.

Thus, based on the obtained results (Table 3), a comparison of the *in vitro* release profiles and dissolution studies of MTF/TPA/GLP/nMCM-48 with Glirum-MF reveals that the designed nanocarrier demonstrates a superior release profile for MTF and GLP compared to the marketed drug. Additionally, it also exhibits a similar pH-dependent release behaviour for the both drugs as observed in case of Glirum-MF.

Table 3 Comparison between dissolution release profile of MTF and GLP from MTF/GLP/TPA/nMCM-48 and Glirum-MF

	% release (*in vitro* study)		% release (dissolution study)	
Drug	pH-1.2	pH-7.4	pH-1.2	pH-7.4
MTF/TPA/GLP/nMCM-48				
MTF	99.9 (8 h)	74.3 (10 h)	99.1 (7.5 h)	80.1 (10 h)
GLP	99.3 (5 h)	99.9 (1.5 h)	95.5 (4 h)	99.4 (2 h)
Glirum-MF				
MTF	99.4 (1 h)	99.9 (1.5 h)	99.9 (2 h)	99.9 (2.5 h)
GLP	99.0 (2 h)	99.9 (0.5 h)	99.9 (2 h)	99.8 (1.5 h)

Release kinetics and mechanism

The drug release kinetics study was performed using various mathematical models (Table 4) such as zero-order, first order and Higuchi model, which describes the drug-release behaviour of both the drugs from MTF/TPA/GLP/nMCM-48. Since GLP and MTF exhibited slower release profiles at pH 1.2 and pH 7.4, respectively, the release kinetics was evaluated by analysing the data obtained under these specific conditions.[18,32,33]

The obtained release studies show that MTF and GLP release follows zero order kinetics followed by Higuchi model of diffusion (Fig. 9).

Diabetes and cancer: a cause of concern

Research shows that individuals with T2DM are significantly more susceptible towards developing various types of cancer, including liver, pancreatic, and breast cancers. The underlying mechanisms (Scheme 3) for this association may involve

Table 4 Mathematical models of drug release[a]

Models	Equation	R^2 value	
		GLP	MTF
Zero order	$Q_t = Q_0 + K_0 t$	0.9843	0.9979
First order	$\log Q_t = \log Q_0 K_1 t/2.303$	0.8397	0.9542
Higuchi	$Q_t = K_H t_{1/2}$	0.9259	0.9927

[a] Where, Q_t is the amount of drug dissolved in time 't' and Q_0 is the initial amount of drug and K_0, K_1 and K_H are the release rate constants, respectively.

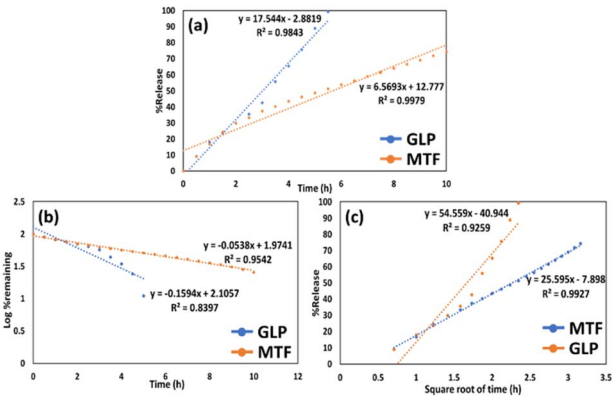

Fig. 9 Release kinetics of GLP and MTF release using (a) zero-order, (b) first order and (c) Higuchi model.

metabolic abnormalities prevalent in T2DM, including hyperinsulinemia and obesity, which can promote cancer cell proliferation and survival.[34–36]

Interestingly, the two commonly prescribed antidiabetic medications, MTF and GLP, have shown potential anticancer effects through distinct mechanisms that primarily involve metabolic regulation and modulation of growth factor signalling pathways.[37–39] MTF primarily acts by reducing insulin resistance and lowering plasma insulin levels, which diminishes the growth stimuli associated with hyperinsulinemia. This reduction in insulin and insulin-like growth factor 1 (IGF-1) levels is crucial because both factors are implicated in promoting cancer cell proliferation and survival. MTF also inhibits the mTOR pathway, a key regulator of cell growth and metabolism, thereby inducing apoptosis in cancer cells and reducing their proliferation, particularly under hyperglycaemic

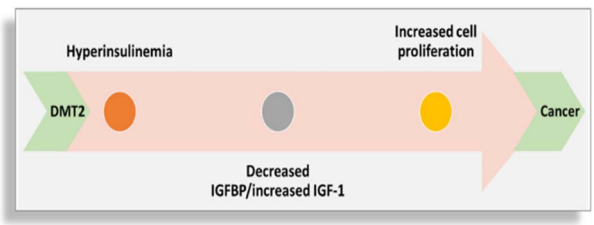

Scheme 3 Schematic representation showing how DMT2 contributes towards cancer development.

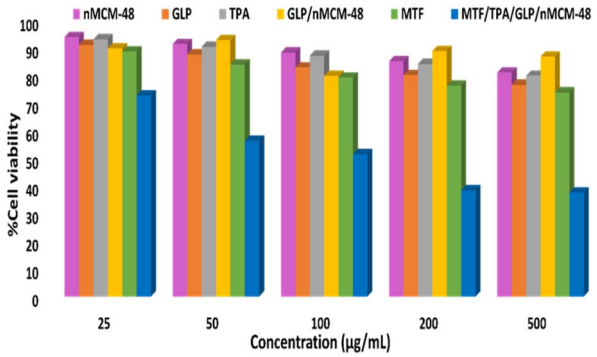

Fig. 10 *In vitro* cytotoxicity assessment.

conditions that favour the Warburg effect, where cancer cells rely on glycolysis for energy production.[40–43]

On the other hand, GLP can inhibit tumour growth and metastasis by interfering with angiogenesis, the process through which new blood vessels form to supply tumours. This effect is mediated through the suppression of the vascular endothelial growth factor (VEGF) signalling pathway, which is critical for angiogenesis.[44–47] Therefore, the use of these medications not only aids in managing diabetes but may also play a role in reducing cancer risk among T2DM patients. In this direction, in the current study MTT assay was carried out using HepG2 cells to evaluate the anticancer potential of the designed nanocarrier.

In vitro cytotoxicity-MTT assay

Fig. 10 illustrates the effects of nMCM-48, GLP, TPA, GLP/nMCM-48, MTF and MTF/TPA/GLP/nMCM-48 on HepG2 cells using MTT assay at various concentrations (25, 50, 100, 200, and 500 µg mL^{-1}). The results showed that nMCM-48 and TPA caused minimal cytotoxicity (≤10%), confirming that the carrier and the capping agent are non-toxic in the tested concentrations. In contrast, GLP, MTF, and GLP/nMCM-48 exhibited slightly higher cytotoxicity (≤15%), with MTF alone reaching efficacy levels of ≥25% at 500 µg mL^{-1}. Notably, the MTF/TPA/GLP/nMCM-48 formulation displayed the most significant cytotoxic effects, with 37% cell viability at the highest concentration of 500 µg mL^{-1}, suggesting enhanced synergistic activity when GLP and MTF are combined. These findings indicate that MTF/TPA/GLP/nMCM-48 could serve as a promising drug delivery system for GLP and MTF, offering increased efficacy, reduced side effects, and improved therapeutic outcomes. This combination may be particularly beneficial for treating T2DM patients with a genetic predisposition to cancer.

Conclusions

To conclude, for the first time a synergistic combination of MTF and GLP was successfully achieved by loading both drugs into a nanocarrier based on nMCM-48 and TPA. *In vitro* release study shows a pH responsive release of both the drugs and a much slower release was obtained from MTF/TPA/GLP/nMCM-48 as

compared to the marketed available formulation, also supported by the *in vitro* dissolution study. Release kinetics study shows that zero order kinetics was followed by Higuchi model of diffusion in case of both of the drugs. Further, taking into account the anticancer potential of both GLP and MTF, MTT assay shows that the designed nanocarrier effectively allowed the co-delivery of dual drug combinations with enhanced synergistic efficacy. Thus, the designed nanocarrier could be effective in combination therapy for diabetes by delivering both the antidiabetic drugs in a pH dependant-controlled manner.

Data availability

Data for this article are available at GitHub repository at **https://github.com/DDG-1997/bookish-octo-enigma.git**.

Author contributions

A. P. conceptualized, supervised, reviewed and edited the final original draft. D. D. carried out the data curation, formal analysis, validation and writing of the original draft.

Conflicts of interest

There are no conflicts to declare.

Acknowledgements

AP and DD are thankful to the Department of Chemistry, The Maharaja Sayajirao University of Baroda for TG-DTA analysis. DD is thankful to SHODH (Scheme of Developing High Quality Research, KCG/SHODH/2022-23/) for providing financial support.

References

1 K. Kupsal, S. Mudigonda, N. V. B. K. Sai, K. Neelala and S. R. Hanumanth, *J. Metab. Syndr.*, 2016, **5**, 210.
2 X. Nie, Z. Chen, L. Pang, L. Wang, H. Jiang, Y. Chen, Z. Zhang, C. Fu, B. Ren and J. Zhang, *Int. J. Nanomed.*, 2020, **15**, 10215–10240.
3 H. M. Manukumar, J. S. Kumar, B. Chandrasekhar, S. Raghava and S. Umesha, *Crit. Rev. Food Sci. Nutr.*, 2017, **57**, 2712–2729.
4 H. Pan, H. Jing, X. Yang, W. Pan and T. Chen, *Drug Dev. Ind. Pharm.*, 2016, **43**, 780–788.
5 Y. Lei, Y. Yan, L. Huang, C. Li, W. Liu, Q. Shen, C. Wang, H. Yang, X. Li, W. Zhang, J. Chen, J. Su, Y. Xie, W. Chen, C. Li, J. Lu and L. Chen, *Int. J. Clin. Pharm. Ther.*, 2024, **2024**, 1–9.
6 D. S. H. Bell, *J. Diabetes Res.*, 2022, **2022**, 1–8.
7 X. Xie, C. Wu, Y. Hao, T. Wang, Y. Yang, P. Cai, Y. Zhang, J. Huang, K. Deng, D. Yan and H. Lin, *Front. Endocrinol.*, 2023, **14**, 1301093.
8 O. Defang, N. Shufang, L. Wei, G. Hong, L. Hui and P. Weisan, *Drug Dev. Ind. Pharm.*, 2005, **31**, 677–685.
9 D. Ouyang, S. Nie, W. Li, H. Guo, H. Liu and W. Pan, *J. Pharm. Pharmacol.*, 2005, **57**, 817–820.
10 S. Abraham, M. Naufal, V. Peter, S. Raju and C. Das, *Asian J. Pharm. Biol. Res.*, 2016, **9**, 235–240.
11 N. Samed, V. Sharma and A. Sundaramurthy, *Appl. Surf. Sci.*, 2018, **449**, 567–573.
12 R. B. Patel, G. N. Patel, H. R. Patel and M. M. Patel, *Drug Dev. Ind. Pharm.*, 2011, **37**, 1244–1252.
13 S. Joshi, M. T. Hussain, C. B. Roces, G. Anderluzzi, E. Kastner, S. Salmaso, D. J. Kirby and Y. Perrie, *Int. J. Pharm.*, 2016, **514**, 160–168.
14 U. Mandal and T. K. Pal, *Drug Dev. Ind. Pharm.*, 2008, **34**, 305–313.
15 S. Pattnaik and K. Swain, *Applications of Nanocomposite Materials in Drug Delivery*, Elsevier, 2018, pp. 589–604.
16 R. Narayan, U. Y. Nayak, A. M. Raichur and S. Garg, *Pharmaceutics*, 2018, **10**, 118.
17 D. Marinheiro, F. Martel, B. J. M. L. Ferreira and A. L. Daniel-da-Silva, *Bioengineering*, 2023, **10**, 40.
18 S. Adhikary, A. Al Hoque, M. Ray, S. Paul, A. Hossain, S. Goswami and R. Dey, *Appl. Biochem. Biotechnol.*, 2023, **195**, 4712–4727.
19 H. Aghaei, A. A. Nourbakhsh, S. Karbasi, R. Javadkalbasi, M. Rafienia, N. Nourbakhsh, S. Bonakdar and K. J. D. MacKenzie, *Ceram. Int.*, 2014, **40**, 7355–7362.
20 Y. Wang, L. Sun, T. Jiang, J. Zhang, C. Zhang, C. Sun, Y. Deng, J. Sun and S. Wang, *Drug Dev. Ind. Pharm.*, 2014, **40**, 819–828.
21 V. Zeleňák, D. Halamová, M. Almáši, L. Žid, A. Zeleňáková and O. Kapusta, *Appl. Surf. Sci.*, 2018, **443**, 525–534.
22 M. B. Čolović, M. Lacković, J. Lalatović, A. S. Mougharbel, U. Kortz and D. Z. Krstić, *Curr. Med. Chem.*, 2019, **27**, 362–379.
23 Z. Ilyas, H. S. Shah, R. Al-Oweini, U. Kortz and J. Iqbal, *Metallomics*, 2014, **6**, 1521–1526.
24 J. Rodrıguez-Gallardo, R. A. Silvestre, E. M. Egido and J. Marco, *Eur. J. Pharmacol.*, 2000, **402**, 199–204.
25 A. Barberà, J. Fernàndez-Alvarez, A. Truc, R. Gomis and J. J. Guinovart, *Diabetologia*, 1997, **40**, 143–149.
26 D. Dasgupta, M. Das, S. Thakore, A. Patel, S. Kumar and S. Seshadri, *J. Drug Deliv. Sci. Technol.*, 2022, **72**, 103419.
27 D. Dasgupta and A. Patel, *Adv. Mater.*, 2022, **3**, 8220–8228.
28 A. Patel and D. Pithadia, *Appl. Catal., A*, 2020, **602**, 117729.
29 S. C. Jagdale, S. A. Patil, B. S. Kuchekar and A. R. Chabukswar, *J. Young Pharm.*, 2011, **3**, 197–204.
30 M. S. Refat, F. M. Al-Azab, H. M. A. Al-Maydama, R. R. Amin, Y. M. S. Jamil and M. I. Kobeasy, *Spectrochim. Acta, Part A*, 2015, **142**, 392–404.
31 S. Kumar, S. Bansal, A. Singh, D. Poddar and A. Sarkar, *Res. Sq.*, 2024, 1–29.
32 M. M. Abdul Hameed, S. A. P. Mohamed Khan, B. M. Thamer, N. Rajkumar, H. El-Hamshary and M. El-Newehy, *Polym. Adv. Technol.*, 2022, **34**, 6–23.
33 M. V. S. Varma, A. M. Kaushal, A. Garg and S. Garg, *Am. J. Drug Deliv.*, 2004, **2**, 43–57.
34 M. Pliszka and L. Szablewski, *Int. J. Mol. Sci.*, 2024, **25**, 7476.
35 B. Zhu and S. Qu, *Front. Endocrinol.*, 2022, **13**, 800995.

36 A. Cortellini, A. D'Alessio, S. Cleary, S. Buti, M. Bersanelli, P. Bordi, G. Tonini, B. Vincenzi, M. Tucci, A. Russo, F. Pantano, M. Russano, L. S. Stucci, M. C. Sergi, M. Falconi, M. A. Zarzana, D. Santini, F. Spagnolo, E. T. Tanda, F. Rastelli, F. C. Giorgi, F. Pergolesi, R. Giusti, M. Filetti, F. Lo Bianco, P. Marchetti, A. Botticelli, A. Gelibter, M. Siringo, M. Ferrari, R. Marconcini, M. G. Vitale, L. Nicolardi, R. Chiari, M. Ghidini, O. Nigro, F. Grossi, M. De Tursi, P. Di Marino, P. Queirolo, S. Bracarda, S. Macrini, A. Inno, F. Zoratto, E. Veltri, C. Spoto, M. G. Vitale, K. Cannita, A. Gennari, D. L. Morganstein, D. Mallardo, L. Nibid, G. Sabarese, L. Brunetti, G. Perrone, P. A. Ascierto, C. Ficorella and D. J. Pinato, *Clin. Cancer Res.*, 2023, **29**, 2714–2724.
37 M. Solhjou, M. R. Sazegar and H. Hamidinezhad, *Appl. Phys. A: Mater. Sci. Process.*, 2024, **130**, 449.
38 C. Qi, Q. Zhou, B. Li, Y. Yang, L. Cao, Y. Ye, J. Li, Y. Ding, H. Wang, J. Wang, X. He, Q. Zhang, T. Lan, K. Ka, H. Lee, W. Li, X. Song, J. Zhou, X. Yang and L. Wang, *Oncotarget*, 2014, **5**, 9966–9979.
39 C. Qi, B. Li, Y. Yang, Y. Yang, J. Li, Q. Zhou, Y. Wen, C. Zeng, L. Zheng, Q. Zhang, J. Li, X. He, J. Zhou, C. Shao and L. Wang, *Sci. Rep.*, 2016, **6**, 27819.
40 Y. Hua, Y. Zheng, Y. Yao, R. Jia, S. Ge and A. Zhuang, *J. Transl. Med.*, 2023, **21**, 403.
41 F. Zi, H. Zi, Y. Li, J. He, Q. Shi and Z. Cai, *Oncol. Lett.*, 2017, **15**, 683–690.
42 P. Saraei, I. Asadi, M. A. Kakar and N. Moradi-Kor, *Cancer Manag. Res.*, 2019, **11**, 3295–3313.
43 M. Daugan, A. Dufaÿ Wojcicki, B. d'Hayer and V. Boudy, *Pharmacol. Res.*, 2016, **113**, 675–685.
44 A. M. Hendriks, D. Schrijnders, N. Kleefstra, E. G. E. de Vries, H. J. G. Bilo, M. Jalving and G. W. D. Landman, *Eur. J. Pharmacol.*, 2019, **861**, 172598.
45 P. Proks, F. Reimann, N. Green, F. Gribble and F. Ashcroft, *Diabetes*, 2002, **51**, S368–S376.
46 A. Olatunde, M. Nigam, R. K. Singh, A. S. Panwar, A. Lasisi, F. A. Alhumaydhi, V. Jyoti kumar, A. P. Mishra and J. Sharifi-Rad, *Cancer Cell Int.*, 2021, **21**, 499.
47 G. Pasello, L. Urso, P. Conte and A. Favaretto, *Oncologist*, 2013, **18**, 1118–1125.